*applied sciences*

MDPI

*Article*

# Brazilian Microalgae-Derived Bioactives: Antioxidant and Antibacterial Properties for Skin Care Application

**Édina A. R. Blasi [1,*], Jamili S. Hofstetter [2], Patrícia Susano [3], Susete Pinteus [3], Alice Martins [3], Helena Gaspar [3,4], Margarida Matias [3,5], Katie Shiels [5], Patrick Murray [5], Thainá I. Lamb [1], Emílio Berghahn [1], Giseli Buffon [1], Anja Reppner [1], Joana Silva [3,*], Celso Alves [3] and João A. P. Henriques [1]**

[1] Graduate Program in Biotechnology, Universidade do Vale do Taquari-Univates, Lajeado 95914-014, Brazil; thaina.lamb@universo.univates.br (T.I.L.); emilio.berghahn@universo.univates.br (E.B.); gisi@universo.univates.br (G.B.); dulliusanja@gmail.com (A.R.); pegas.henriques@gmail.com (J.A.P.H.)
[2] Life Sciences Area, Universidade do Vale do Taquari-Univates, Lajeado 95914-014, Brazil; jamili.hofstetter@universo.univates.br
[3] MARE-Marine and Environmental Sciences Centre & ARNET—Aquatic Research Network Associated Laboratory, School of Tourism and Maritime Technology (ESTM), Polytechnic University of Leiria, 2520-630 Peniche, Portugal; patricia.f.susano@ipleiria.pt (P.S.); susete.pinteus@ipleiria.pt (S.P.); alice.martins@ipleiria.pt (A.M.); hmgaspar@fc.ul.pt (H.G.); margarida.matias@tus.ie (M.M.); celso.alves@ipleiria.pt (C.A.)
[4] BioISI-Biosystems and Integrative Sciences Institute, Faculty of Sciences, University of Lisbon, 1749-016 Lisboa, Portugal
[5] Shannon Applied Biotechnology Research Centre, TUS, Moylish Park, V94 E8YF Limerick, Ireland; katie.shiels@tus.ie (K.S.); patrick.murray@tus.ie (P.M.)
* Correspondence: edinablasi@gmail.com (É.A.R.B.); joana.m.silva@ipleiria.pt (J.S.)

## Abstract

Brazilian microalgae represent an underexplored reservoir of bioactive compounds with promising biotechnological and dermocosmetic applications. In this study, eight native Brazilian microalgae strains were cultivated under control (C) and stress conditions, nitrogen depletion (N) and salt stress (S), to modulate their bioactive profiles. Derived acetone extracts (24 samples) were evaluated for their antioxidant and antibacterial activities relevant to skin health. The antioxidant capacity of extracts was assessed by three complementary methods: ferric reducing antioxidant power (FRAP), 2,2-diphenyl-1-picrylhydrazyl (DPPH) and superoxide anion radicals scavenging. Additionally, the antibacterial effects against four skin microorganisms (*Staphylococcus epidermidis*, *Staphylococcus hominis*, *Staphylococcus aureus*, and *Cutibacterium acnes*) were also assessed. Among the tested samples, extracts from *Scenedesmus armatus* (Extract 40C) and from *Chlorella sorokiniana* (Extract 198C) displayed the highest antioxidant potential, with DPPH radical reduction of 22.6 ± 1.6% and 20.7 ± 1.9% and FRAP values of 178.3 and 156.8 µmol $FeSO_4$/g extract, respectively. Superoxide scavenging assays showed $IC_{50}$ values of 150.9 µg/mL for sample 40C and 139.6 µg/mL for sample 198C. Regarding the antibacterial assay, the $IC_{50}$ values for *S. epidermidis* were notable, with sample 198C exhibiting the highest potency (10.3 µg/mL), closely matching the standard drug (12.4 µg/mL). The inhibitory capacity against *C. acnes* showed that samples 40C (58.4 µg/mL) and 198C (83.5 µg/mL) demonstrated antimicrobial relevance. Mechanistic assays suggested that the antibacterial effects of both samples may involve alterations in bacterial membrane integrity and DNA damage. Overall, these findings highlight the dermocosmetic potential of native Brazilian microalgae, still largely untapped in biotechnology, as natural sources of multifunctional ingredients for the development of sustainable skin care formulations.



Academic Editors: Anna Muzykiewicz-Szymańska, Karolina Jakubczyk and Anna Nowak

Received: 9 January 2026
Revised: 4 February 2026
Accepted: 12 February 2026
Published: 23 February 2026

**Keywords:** *Chlorella sorokiniana*; *Cutibacterium acnes*; *Scenedesmus armatus*; *Staphylococcus epidermidis*; membrane and DNA damage; nature-derived functional cosmetics

## 1. Introduction

Microalgae are photosynthetic microorganisms widely distributed across aquatic and terrestrial environments and constitute the base of aquatic food webs, contributing approximately 40% of global productivity [1,2]. Their ability to thrive under extreme conditions has been associated with the production of a wide range of bioactive compounds, positioning microalgae as promising resources for biotechnological applications [3].

Brazilian territory, one of the greatest reservoirs of biodiversity worldwide, includes six of the main continental biomes and a wide range of marine and coastal ecosystems [4]. This diversity is reflected in its algal flora, with nearly 5000 described species, including a significant number of microalgae with recognized biotechnological potential [5,6]. Despite growing interest in microalgal biotechnology, studies specifically addressing the bioactive potential of native Brazilian microalgal strains remain limited, particularly regarding their application in the pharmaceutical and cosmetic sectors [7]. Nonetheless, preliminary studies suggest that these species may harbor antioxidant and antimicrobial compounds with promising applications in functional dermocosmetic formulations [8].

Microalgae are known to biosynthesize several classes of bioactive compounds, including polyunsaturated fatty acids (PUFAs), pigments (chlorophylls and carotenoids), proteins, peptides, vitamins, exopolysaccharides, and phytohormones, among others [9]. Many of these compounds exhibit antimicrobial, antioxidant, and anti-inflammatory activities, which are highly relevant for skin health and cosmetic applications [10,11]. In dermocosmetics, such properties are associated with anti-aging effects, photoprotection, skin barrier reinforcement, and the prevention or mitigation of inflammatory skin conditions.

Skin-associated microorganisms, such as species from the genera *Staphylococcus* and *Cutibacterium*, play a crucial role in skin homeostasis but may also be involved in the development of pathological conditions when microbial balance is disrupted [12–18]. The increasing prevalence of antimicrobial resistance and skin dysbiosis highlights the need for alternative, naturally derived antimicrobial agents. Microalgal compounds, especially PUFAs, have demonstrated antibacterial activity against several skin-related microorganisms, reinforcing their potential as sustainable bioactive ingredients [19–22].

In addition to their bioactive potential, microalgae represent a renewable and environmentally sustainable resource, offering advantages such as high biomass productivity, low freshwater requirements, $CO_2$ mitigation capacity, and adaptability to controlled cultivation systems [20–24]. Although microalgae in Brazil have been predominantly explored for biofuel production and wastewater treatment, their application as a source of high-value bioactive compounds remains underexplored [25]. Therefore, the main objective of this study was to evaluate the antioxidant and antibacterial activities of components derived from eight microalgae species from the Syntalgae culture collection company (Lajeado, Rio Grande do Sul, Brazil) for their potential use in sustainable dermatological and cosmetic formulations.

## 2. Materials and Methods

### 2.1. Microalgae Cultivation and Processing

The microalgae tested in this study were collected in Brazil between January 2021 and March 2022 at different locations, specifically from the states of Rio Grande do Sul, Santa Catarina, Paraná, and Ceará. The reagents and materials used for culture media preparation

and other applications were purchased from Labsynth Produtos, Laboratórios Ltd., Diadema, Brazil. The enrichment culture technique was used for the isolation process, in which 50 mL of the sample was centrifuged at 2000× *g* for 1 min (Novatécnica Indústria e Comércio de Equipamentos para Laboratório, Piracicaba, Brazil The supernatant was subsequently discarded and the pellet resuspended in standard culture media BBM (Bold's Basal Medium) [26–28], BG-11 (Blue-Green Algae Medium) [29–31], and TAP (Tris-Acetate-Phosphate) [28,32–34], with slight modifications, and then incubated in a Solab SL-221/300-E-F Biochemical Oxygen Demand (BOD) growth chamber (Solab Equipamentos para Laboratórios, Piracicaba, Brazil) for 14 days. After this period, aliquots of 50 µL of the culture were spread on Petri dishes containing the respective solid culture media, using a Drigalski loop. From these plates, isolated colonies were streaked onto new plates using a platinum loop.

The microalgae were grown in the BOD chamber at 25 °C with a light/dark cycle of 16 h/8 h. A photon flux density of 55 µmol $m^{-2}s^{-1}$ was used for Petri dishes and liquid cultures of less than 100 mL. For liquid cultures over 100 mL, a photon flux density of 80–120 µmol $m^{-2}s^{-1}$ was used [35]. After isolation, the microalgae were assigned numerical identifiers based on the sequence of isolations in Syntalgae company's strain bank: SYN 07, SYN 27, SYN 33, SYN 40, SYN 41, SYN 63, SYN 198, and SYN 211.

### *2.2. Identification of Isolates by Microscopy and Sequencing of the 18S rDNA Gene and ITS Regions*

The morphological study was conducted using solid culture material under an optical microscope (Nikon Eclipse Ei and Nikon Eclipse E200, Sendai Nikon Corporation, Natori, Japan). The following morphological criteria were examined: cell shape, color, and arrangement of sheaths; type of cell division; uniformity of the contents; and organization of the interior of the cells. The key to the genera of algae from Brazilian continental waters was used for identification [36].

Molecular analyses were performed with genomic DNA isolated from the microalgae strains using the PureLink™ Genomic Plant DNA Purification Kit (Invitrogen Brasil Ltd., São Paulo, Brazil) or a protocol containing cetyltrimethylammonium bromide (CTAB) and polyvinylpyrrolidone (PVP) [37]. In this case, the DNA obtained was resuspended in 50 µL of 10 mM Tris-HCl, pH 8.0, and 1 mM EDTA and then stored at −20 °C. The isolated DNA was used as a template for the amplification of the 18S rRNA gene using primers P2 (5′-CTGGTTGATTCTGCCAGT-3′) and P4 (5′-TGATCCTTCYGCAGGTTCAC-3′) [38]. PCR was performed using approximately 10 ng of DNA, 500 nM of each primer, 250 nM triphosphate deoxyribonucleotides (dNTP), 1.5 mM magnesium chloride ($MgCl_2$) and 1 unit of Platinum™ Taq DNA Polymerase (Invitrogen Brasil Ltd.a, São Paulo, Brazil). The parameters used in the thermal cycler (TC-512, TECHNE, Chelmsford, UK) were denaturation at 94 °C for 5 min, followed by 35 cycles of denaturation at 94 °C for 30 s, annealing at 55 °C for 30 s, and extension at 72 °C for 2 min, with a final extension of 10 min at 72 °C [39]. In order to amplify the ITS regions, primers ITS1f (5′-AGGAGAAGTCGTAACAAGGT-3′), ITS2r (5′-GCTGCGTTCTTCATCGATGC-3′), ITS3f (5′-GCATCGATGAA-GAACGCAGC-3′), and ITS4r (5′-TCCTCCGCTTATTGATATGC-3′) [40] were used. The conditions applied for the PCR were: denaturation at 94 °C for 5 min, followed by 35 cycles of denaturation at 94 °C for 30 s, annealing at 55 °C for 30 s, and extension at 72 °C for 1 min, followed by a final 10 min extension at 72 °C [41].

The sequences of the 18S rDNA gene and the ITS regions obtained using the Sanger method were aligned using the ClustalW 2.1 program and compared with the sequences available in the National Center for Biotechnology Information (NCBI) database using the BLASTN 2.0.5 program. The identification of the strains was based on both morphological and molecular criteria. For molecular identification, the selection of primers was guided by the protocol described by Fawley and Fawley (2020) [42]. The assignment of strains

to a specific genus or species was based on the highest percentage of identity and the lowest E-values, following the parameters established in Fawley and Fawley (2020) [42]. Only matches with a percentage identity $\geq$ 98% for 18S rRNA and $\geq$99% for ITS regions were considered conclusive for species-level identification. This approach enabled the identification of the isolated strains at the genus or species level.

### 2.3. Biomass Production Under Control and Stress Conditions

Herein, the microalgae strains were studied for their ability to produce bioactive substances under control conditions (C) or under stress with total nitrogen deficiency (N) and 2% NaCl (S). Letters in brackets accompany the sample numbers, indicating the growth condition of each sample, for example: 40C, 40S, and 40N. The cultures were inoculated into test tubes containing 10 mL of standard liquid medium and incubated in the BOD chamber for approximately one week without shaking under the light and temperature conditions previously described for isolation. Subsequently, the cultures were transferred to 125 mL Erlenmeyer flasks containing 10 mL of inoculum, 2.5 mL of glucose (200 g/L), and 37.5 mL of liquid medium and placed under constant agitation at 170.05 rpm in a Solab SL-223 shaker incubator (Solab Equipamentos para Laboratórios, Piracicaba, Brazil). At the end of the exponential growth phase (+/− 7 days), the biomass generated was passed on to the stress condition, except for the control sample, which was centrifuged (Novatecnica NT-835, Novatécnica Indústria e Comércio de Equipamentos para Laboratório, Piracicaba, Brazil) and stored. For N stress, the samples were centrifuged at 5000× *g* for 15 min and washed with modified culture medium (N off) and then re-inoculated in 125 mL Erlenmeyer flasks with 50 mL of the same medium. For salt stress experiments, only a saline solution was added to achieve a final concentration of 2% NaCl in the culture. Both conditions were maintained under constant agitation at 170 rpm. After an additional 7 days, the cultures were centrifuged at 5000× *g* for 10 min. The supernatant was discarded, and the resulting biomass was stored at −20 °C for later analysis or freeze-drying [43,44].

### 2.4. Preparation of Microalgae Extracts

To obtain the extracts, 1 g of freeze-dried biomass was mixed with 15 mL of HPLC-grade acetone (Honeywell Riedel-de Haën, Seelze, Germany). Acetone was selected as the extraction solvent because it is widely recognized as an efficient solvent for recovering a broad range of microalgal metabolites, including pigments, lipids, and moderately polar secondary metabolites. Its intermediate polarity enables the simultaneous extraction of both polar and non-polar bioactive compounds, making it particularly suitable for untargeted metabolite profiling of microalgal biomass. Additionally, acetone penetrates microalgal cell walls effectively and is easily removed due to its low boiling point. The use of HPLC-grade acetone is important to minimize contamination from solvent impurities that could interfere with downstream analytical techniques such as LC–MS and NMR. Lower-grade solvents may contain trace organic residues that can produce background peaks, suppress ionization in mass spectrometry, or introduce misleading signals in spectroscopic analyses.

The extraction was performed through 15 sequential cycles, each consisting of the following steps: (1) addition of 15 mL of acetone; (2) vortex mixing for 30 s; (3) sonication for 5 min in a Branson S250 (Branson Ultrasonic, Barcelona, Spain) sonicator (10% amplitude), performed twice per cycle; (4) centrifugation for 10 min at 5000× *g* and 15 °C (Eppendorf 5810R centrifuge, Hamburg, Germany). After each cycle, the supernatant was collected and filtered through filter paper (12 to 15 µm, Fisher Scientific, Porto Salvo, Portugal). All supernatants were pooled, and the solvent was evaporated under vacuum at 35–40 °C using a Heidolph Laborota 4000 (Heidolph Instruments GmbH & Co. KG, Schwabach, Germany) rotary evaporator (120 rpm). At the end of the process, the extract was transferred

to previously pre-weighed glass tubes and left in an exhaust hood until all the solvent had completely evaporated. The final dryness was achieved in a speed-vac equipment (Eppendorf Concentrator Plus, Leicestershire, UK). The tubes were then reweighed to obtain the yield (mg) of dry extract [45].

### 2.5. Determination of Extracts' Antioxidant Capacity

The antioxidant capacity of the microalgae extracts was assessed using three different methods: scavenging of the 2,2-diphenyl-1-picrylhydrazyl (DPPH) and superoxide radical ($O_2^{\bullet-}$), and the ferric reducing antioxidant power (FRAP). The negative control was prepared using the highest concentration of dimethyl sulfoxide (DMSO) as the vehicle. Ascorbic acid (AA), 3,5-di-*tert*-4-butylhydroxytoluene (BHT), and quercetin (QUE) were used as positive controls. All sample analyses were carried out in triplicate across three independent experiments.

#### 2.5.1. 2,2-Diphenyl-1-Picrylhydrazyl Radical (DPPH) Scavenging Method

The capacity of the microalgae extracts (at a concentration of 200 µg/mL) to reduce the DPPH radical was determined according to the procedure described by Brand-Williams, Cuvelier and Berset [46] with slight modifications described by Silva, J. et al. [47]. Briefly, 198 µL of DPPH radical solution (Sigma -Aldrich, Indian, Bengalore) [0.1 mM], previously prepared in absolute ethanol, was added to the microalgae extracts (Cstock: 20 mg/mL; 2 µL) in 96-well plates. After 30 min in the dark, the plates were read in a microplate reader (Multimodal Synergy H1, BioTek® Instruments, Winooski, VT, USA), and the absorbance was measured at 517 nm. The results are presented as a percentage of control.

#### 2.5.2. Ferric Reducing Antioxidant Power (FRAP)

The FRAP assay was carried out as described by Benzie and Strain [48], adapted to the microscale. This method is based on the reduction of $Fe^{3+}$ to $Fe^{2+}$ through electron donation, which can be mediated by the presence of antioxidant compounds, leading to the formation of an intense blue color proportional to the antioxidant activity. The FRAP reagent was prepared by combining 0.3 M sodium acetate buffer (pH 3.6), 10 mM 2,4,6-tris(2-pyridyl)-*s*-triazine (TPTZ) (TCI, Shimoyama, Miizugahara, Kumagaya City, Saitama, Japan), and 20 mM ferric solution ($FeCl_3$) (Sigma-Aldrich, Saint Louis, MO, USA) in a 10:1:1 ratio, then incubated at 37 °C. Next, 198 µL of the FRAP reagent was added to the microalgae extracts (2 µL, at a concentration of 100 µg/mL), which were then incubated in the dark for 30 min. After this time, the absorbance was measured at 593 nm (Multimodal Synergy H1, BioTek® Instruments, Winooski, VT, USA). $FeSO_4$ was used as a standard in the calibration curve, and the results were expressed as µmol $FeSO_4$/g of extract.

#### 2.5.3. Superoxide Radical Scavenging Activity

The scavenging activity of the superoxide radical ($O_2^{\bullet-}$) evaluates its reduction by antioxidants. The superoxide radical is produced at the junction of *N*-methylphenazine methosulfate (PMS) (Sigma-Aldrich, Saint Louis, MO, USA) and NADH (a reduced form of nicotinamide-adenine dinucleotide) (Sigma-Aldrich, Saint Louis, MO, USA), which reduces nitro blue tetrazolium chloride (NBT) (TCI, Shimoyama, Miizugahara, Kumagaya City, Saitama) in the presence of dissolved oxygen. It is possible to observe the consumption of $O_2^{\bullet-}$ in the reaction mixture when there is a decrease in absorbance in the presence of antioxidant molecules [49] Solutions of NADH (0.557 mM), PMS (0.450 mM, prepared from a 10 mM stock solution), and NBT (0.108 mM) were prepared in Tris-HCl (16 mM, pH = 8.0). The 96-well plate was then prepared by mixing the microalgae extracts (200 µg/mL) with the three solutions in the respective wells. For the blanks, Tris-HCl was added as an alternative to PMS, followed by a 5 min incubation, and the absorbance was measured

at 560 nm (Multimodal Synergy H1, BioTek® Instruments, Winooski, VT, USA) [50]. The radical scavenging capacity was calculated using the following equation:

$$\text{Radical scavenging activity (\%control)} = \frac{\text{Abs sample} - \text{Abs blank}}{\text{Abs control}} \times 100$$

where Abs sample is the absorbance of the samples with PMS, Abs blank is the absorbance of the samples with Tris-HCl, and Abs control is the absorbance of the solutions with DMSO. For the extracts that reduced the $O_2^{\bullet -}$ radical by more than 50% at the maximum concentration (200 µg/mL), the $EC_{50}$ values (µg/mL) were determined by testing the concentrations of 10, 30, 60, and 100 µg/mL.

### 2.6. In Vitro Antibacterial Capacity

Antibacterial activity was tested against the following microorganisms: *Cutibacterium acnes* (DSM 1897), *Staphylococcus aureus* (DSM 1104), *Staphylococcus epidermidis* (DSM 1798), and *Staphylococcus hominis* (DSM 20329), from the German Collection of Microorganisms and Cell Cultures (DSMZ). Trypticase Soy Broth medium with 0.3% yeast extract was used for the growth of *S. epidermidis* and *S. hominis*. For the growth of *C. acnes*, Trypticase Soy Broth medium was used under anaerobic conditions. Finally, Luria Broth medium was used for the growth of *S. aureus* [50].

The extracts were tested initially at 200 µg/mL. Controls were performed with the highest concentration of DMSO (vehicle), and all analyses were carried out in triplicate. A freshly overnight culture of each microorganism was used in the assays. The initial inoculum was adjusted to 0.5 MacFarland scale, after which 198 µL were placed in a 96-well plate, following the addition of 2 µL of each extract. The plates were then incubated at 37 °C for approximately 4 h for *S. aureus*, *S. epidermidis*, and *S. hominis* and 72 h for *C. acnes* (exponential growth phase of each microorganism). Growth was monitored spectrophotometrically at 600 nm (Multimodal Synergy H1, BioTek® Instruments, Winooski, VT, USA), and the results were expressed as a percentage of the vehicle, as follows:

$$\text{Inhibitory activity}(\%) = 100 - \left( \frac{\text{Abs sample (T1} - \text{T0)}}{\text{Abs vehicle (T1} - \text{T0)}} \times 100 \right)$$

where T0 is the absorbance at inoculation time, and T1 is the absorbance after incubation time.

For the extracts that reduced bacterial growth by more than 50% at 200 µg/mL, a dose–response analysis was conducted to determine the $IC_{50}$ values, testing a range of concentrations between 0.3 and 100 µg/mL.

### 2.7. Mechanisms of Action Underlying the Antimicrobial Activity

To understand the mechanisms that could be underlying the antimicrobial effects, further tests were conducted with the most active extracts. The extracts were dissolved at a stock concentration of 20 mg/mL.

#### 2.7.1. Membrane Damage Assay

Membrane damage analysis was performed according to Pinteus et al. [51], as follows: a freshly overnight-grown culture was centrifuged (2000× *g*, 5 min) and adjusted to 1 MacFarland scale. Extracts were added at 200 µg/mL and incubated for 4 h at 37 °C for *S. epidermidis* and for 6 h for *C. acnes*. DMSO was used as a negative control (vehicle). Blanks were prepared with samples without the microorganism. Positive control was prepared by applying a thermic treatment (100 °C, 10 min) to induce total membrane permeability. All suspensions were transferred to a black microplate and incubated with 2 µM Sytox

Green probe (Thermo Fisher Scientific, Waltham, MA, USA) for 10 min in the microplate reader. The resultant fluorescence of the DNA-bound dye was quantified on a fluorescence microplate reader (Multimodal Synergy H1, BioTek® Instruments, Winooski, VT, USA). The membrane damage was determined in % of positive control (thermic treatment), discounting blanks and DMSO fluorescence.

#### 2.7.2. DNA-Damaging Potential

The DNA-damaging potential was assessed following the methodology described by Pinteus et al. [51]. Plasmid (pGADT7—7987 bp) DNA (5 µL; 100 ng) was mixed with microalgae extracts (2 µL; 2 mg/mL) and ultrapure water (13 µL). The reaction mixture was incubated at 37 °C for 1 h before being loaded onto a 0.8% agarose gel containing 1% RedSafe™. Gene Ruler 1 Kb DNA Ladder (5 µL) (Thermo Fisher Scientific, Vilnius, Lithuania) was also loaded onto the gel. Electrophoresis was then performed for 45 min under 85 V. DMSO (2 µL) and ciprofloxacin (2 µL; 1 µg/mL) were used as negative and positive controls, respectively.

### *2.8. Chemical Characterization*

A chemical screening of the two most bioactive microalgae extracts was performed by proton nuclear magnetic resonance spectroscopy ($^1$H NMR) and ultraviolet–visible spectrophotometry (UV-Vis). Additionally, liquid chromatography coupled to mass spectrometry (LC-MS) was used to identify the fatty acid composition of both samples.

#### 2.8.1. UV-Vis Analysis

The UV-Vis absorption spectra of samples were measured on an Evolution 201 UV-Vis spectrophotometer (Thermo Scientific, Madison, WI, USA) in the 200–800 nm wavelength range. For this purpose, samples were dissolved (1 mg/mL) in HPLC-grade acetone (VWR-BDH Chemicals, Rosny-sous-Bois, France).

#### 2.8.2. $^1$H NMR Analysis

For NMR analysis, samples (c.a. 5–6 mg) were dissolved in 0.5 mL of deuterated acetone (Sigma-Aldrich, St. Louis, MO, USA) and the $^1$H NMR spectra were recorded at 400.13 MHz on a Bruker AMX400 spectrometer (Bruker BioSpin GmbH, Rheinstetten, Germany) at 25 °C. Chemical shifts (δ) are expressed in ppm and referenced to the residual solvent signal ($\delta_H$ = 2.09).

#### 2.8.3. LC-MS Analysis of Fatty Acids

The fatty acid profile of both samples was determined using the method previously described by Saha et al. [52]. Samples were reconstituted in 500 µL of dichloromethane: methanol (1:2, *v*/*v*), and the content was centrifuged for 6 min at 16,250× *g* using a Heraeus Biofuge Stratos centrifuge (Fisher Scientific Ltd., Dublin, Ireland). The supernatant was then filtered through Sartorius Minisart Syringe Filters (0.2 µm, 15 mm PTFE) and 10 µL were injected into an HPLC equipped with a Q-TOF mass spectrometer (Agilent 6520, Agilent Technologies, Cork, Ireland) using electrospray ionization (ESI). Analytes were resolved by an Agilent C-18 Poroshell 120 column (2.7 µm, 3.0 × 150 mm) with gradient elution. Mobile phase A consisted of 2 mM ammonium acetate in water, and mobile phase B consisted of 2 mM ammonium acetate in 95% (*v*/*v*) acetonitrile. The flow rate of the mobile phase started at 0.3 mL/min for the first 5 min, increased to 0.6 mL/min after 10 min, and was maintained at this rate for the remainder of the run. The mass spectrometer was operated in negative ionization mode, scanning from 50 to 1100 *m*/*z*. Drying gas flow rate, temperature, and nebuliser pressure were 5 L/min, 325 °C, and 30 psi, respectively. Fragmentor and skimmer voltages were maintained at 175 and 65 V, respectively, with a capillary voltage of 3500 V.

### 2.9. Data and Statistical Analysis

The results are presented as the mean ± standard error of the mean (SEM). At least three independent experiments, carried out in triplicate, were performed. The analyses involved more than three groups, so one-way analysis of variance (ANOVA) followed by Dunnett's multiple comparison test was performed to assess significant differences relative to the control treatment. Data normality was evaluated using the Shapiro–Wilk test. Comparisons concerning variables that did not meet variance or distributional assumptions were carried out with Kruskal–Wallis non-parametric test. Statistical significance was set at $p < 0.05$. Additionally, the half-maximal effective/inhibitory concentration ($EC_{50}/IC_{50}$) values were calculated using the GraphPad Prism (v8.0; GraphPad software, San Diego, CA, USA). Dose–response curves were generated from 5 tested concentrations of each extract and fitted by non-linear regression using a four-parameter logistic (4PL) model. The 95% confidence intervals (CI95%) were calculated by the software based on the standard error of the regression. In all assays, $IC_{50}/EC_{50}$ values were determined for all samples showing measurable activity. Compounds that did not show activity within the tested range (e.g., ascorbic acid and BHT in the superoxide scavenging assay) were used only as assay references, and no $IC_{50}$ values were calculated.

## 3. Results

### 3.1. Microalgae Isolation and Molecular Identification

Eight strains of microalgae were selected from the Syntalgae company's isolate bank and identified as SYN 07, SYN 27, SYN 33, SYN 40, SYN 41, SYN 63, SYN 198 and SYN 211. The molecular identification approach revealed that the selected strains belong to the following species (Figure 1): *Chlorella sorokiniana* (SYN 07 and SYN 198), *Desmodesmus insignis* (SYN 27), *Scenedesmus armatus* (SYN 40), *Coelastrella tenuitheca* (SYN 63 and SYN 211), *Graesiella emersonii* (SYN 41), and *Graesiella* sp. (SYN 33).

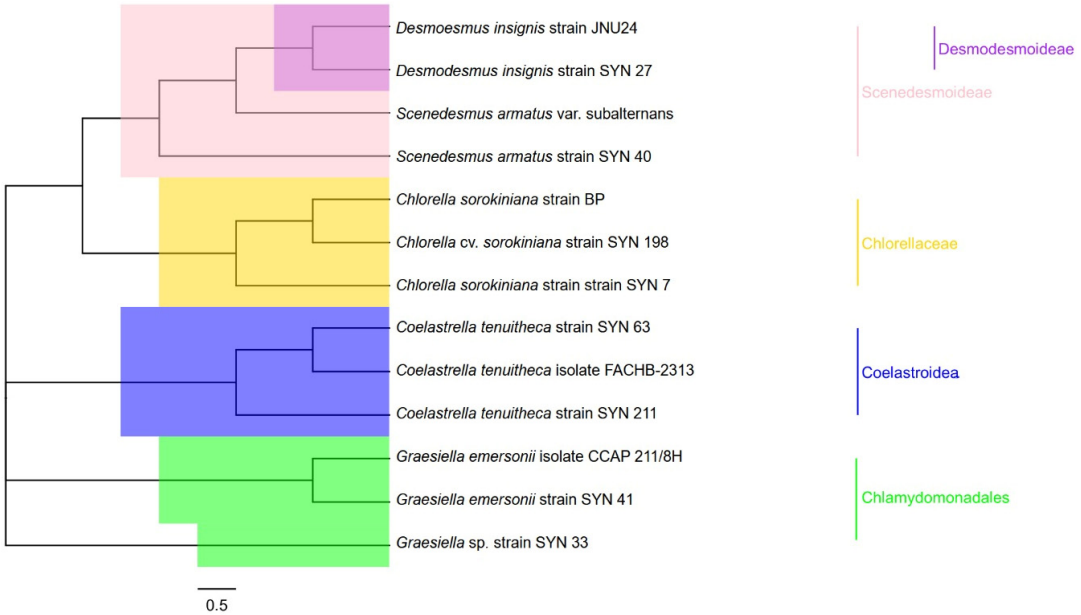


**Figure 1.** Evolutionary relationships of the taxa. Evolutionary history was inferred using the Neighbor-Joining method [53]. The optimal tree is shown. The percentage of replicate trees in which the associated taxa clustered together in the bootstrap test (1000 replicates) [54]. The evolutionary distances were computed using the Maximum Composite Likelihood method [55] and are in the units of the number of base substitutions per site. This analysis involved 13 nucleotide sequences. All ambiguous positions were removed for each sequence pair (pairwise deletion option). There were a total of 2779 positions in the final dataset. Evolutionary analyses were conducted in MEGA11 [56].

### 3.2. Antioxidant Capacity

Concerning the antioxidant capacity (Table 1), most microalgae extracts revealed great capacity to reduce the superoxide radical by more than 50%. Consequently, dose–response analyses were conducted to determine the $EC_{50}$ value (µg/mL), with samples 07C and 33S exhibiting the highest activity ($EC_{50}$ values, 120.3 and 128.8 µg/mL, respectively). Regarding the FRAP method, the extracts that showed the greatest capacity to reduce the Fe (III) ion were *Scenedesmus armatus* (40C) and *Chlorella sorokiniana* (198C) with values of 178.3 µmol and 156.8 µmol of $FeSO_4$/g of extract, respectively, as well as 198S with 102.1 µmol of $FeSO_4$/g of extract. In the DPPH assay, the greatest capacity was also mediated by the 198C and 40C extracts, exhibiting a reduction of 20.7% and 22.6%, respectively.

**Table 1.** Antioxidant capacity of microalgae extracts, and standard antioxidants (AA, BHT and QUE) evaluated by distinct assays, namely the scavenging of the DPPH and superoxide radicals and ferric reducing antioxidant power (FRAP).

| Extract | DPPH [a] (% of reduction) | FRAP [b] | Superoxide Radical [c] |
|---|---|---|---|
| 33C | 6.4 ± 1.0 | 63.3 ± 3.5 | 181.8 (164.4–204.1) |
| 33S | 1.2 ± 1.1 | 70.0 ± 9.1 | 128.8 (123.0–134.9) |
| 33N | 1.6 ± 0.3 | 12.8 ± 3.0 | 195.7 (180.0–215.7) |
| 41C | 0.8 ± 0.7 | 55.2 ± 10.4 | 158.3 (147.2–171.0) |
| 41S | 2.2 ± 0.7 | 16.9 ± 6.7 | 198.4 (183.7–216.9) |
| 41N | 5.0 ± 0.8 | 46.0 ± 1.5 | 144.9 (135.0–156.1) |
| 63C | 2.7 ± 0.6 | 53.0 ± 3.4 | 139.1 (130.8–148.1) |
| 63S | 0.0 ± 0.4 | 10.9 ± 1.3 | 183.0 (173.0–192.9) |
| 63N | 2.3 ± 0.3 | 9.5 ± 2.6 | 132.2 (124.7–140.3) |
| 211C | 11.2 ± 1.3 | 48.5 ± 3.1 | 176.7 (164.3–190.1) |
| 211S | 0.0 ± 0.6 | 21.1 ± 2.9 | >200 |
| 211N | 1.5 ± 0.4 | 45.8 ± 6.2 | >200 |
| 07C | 3.3 ± 0.8 | 41.1 ± 2.8 | 120.3 (111.6–129.9) |
| 07S | 2.3 ± 0.6 | 6.8 ± 2.5 | 184.0 (172.5–196.9) |
| 07N | 1.0 ± 0.4 | 17.6 ± 5.1 | 140.0 (131.7–149.0) |
| 198C | 20.7 ± 1.9 | 156.8 ± 14.8 | 139.6 (132.2–147.6) |
| 198S | 8.4 ± 0.8 | 102.1 ± 5.6 | 149.1 (142.4–156.3) |
| 198N | 13.6 ± 1.8 | 46.1 ± 5.8 | 142.2 (130.4–155.9) |
| 27C | 13.3 ± 2.0 | 88.9 ± 13.3 | 152.3 (144.0–161.5) |
| 27S | 2.9 ± 0.5 | 83.2 ± 9.6 | 172.9 (165.4–181.0) |
| 27N | 10.6 ± 1.6 | 61.0 ± 9.4 | 182.9 (174.1–192.6) |
| 40C | 22.6 ± 1.6 | 178.3 ± 9.9 | 150.9 (144.2–158.3) |
| 40S | 2.9 ± 0.3 | 52.0 ± 6.0 | >200 |
| 40N | 10.9 ± 0.5 | 25.4 ± 3.9 | 186.2 (173.3–201.0) |
| AA | 95.0 ± 0.6 | 21,059.0 ± 213.9 | - |
| BHT | 21.3 ± 1.7 | 8,898.0 ± 242.8 | - |
| QUE | - | - | 5.0 (4.5–5.4) |

[a] DPPH radical scavenging activity (% of reduction) at 200 µg/mL; [b] µmol of $FeSO_4$ equivalents/g extract (µmol $FeSO_4$/g); [c] Scavenging superoxide radical activity ($EC_{50}$ µg/mL). $EC_{50}$ values are expressed as confidence intervals (CI95%). Values in parentheses correspond to the 95% confidence intervals calculated by non-linear regression analysis using GraphPad Prim. DPPH and FRAP values represent mean ± std. error of mean (SEM). AA (ascorbic acid); BHT (3,5-di-t*ert*-4-butylhydroxytoluene); QUE (quercetin).

### 3.3. Antibacterial Activity

The antibacterial effects of microalgae-derived extracts are shown in Table 2. The data obtained displays the ability of the microalgae extracts to reduce the growth of *C. acnes*, *S. aureus*, *S. hominis*, and *S. epidermidis*.

**Table 2.** Antibacterial activity of microalgae-derived extracts ($IC_{50}$ value; 0.3–100 µg/mL) and reference antimicrobial drug (oxytetracycline (0.003–100 µg/mL)) against *Cutibacterium acnes*, *Staphylococcus aureus*, *Staphylococcus hominis*, and *Staphylococcus epidermidis*.

| Extract | *Cutibacterium acnes* | *Staphylococcus epidermidis* | *Staphylococcus hominis* | *Staphylococcus aureus* |
|---|---|---|---|---|
| | | ($IC_{50}$ µg/mL) | | |
| 33C | 118.8 (106.6–132.4) | 31.3 (22.4–43.8) | >200 | >200 |
| 33S | >200 | >200 | >200 | >200 |
| 33N | 147.2 (131.6–164.7) | >200 | >200 | >200 |
| 41C | 152.3 (125.6–184.8) | 42.2 (30.9–57.6) | >200 | >200 |
| 41S | 158.9 (135.1–186.8) | 125.2 (93.0–168.4) | >200 | >200 |
| 41N | 85.2 (68.4–106.1) | 49.7 (40.1–61.7) | >200 | >200 |
| 63C | 129.7 (114.5–147.0) | 104.8 (90.0–122.0) | >200 | >200 |
| 63S | >200 | >200 | >200 | >200 |
| 63N | 148.5 (130.6–168.8) | 124.6 (105.5–147.1) | >200 | >200 |
| 211C | 144.6 (126.7–165.0) | 91.9 (65.1–130.0) | >200 | >200 |
| 211S | >200 | >200 | >200 | >200 |
| 211N | 126.6 (113.2–141.7) | >200 | >200 | >200 |
| 07C | 93.9 (80.5–109.4) | 40.3 (28.2–57.7) | >200 | >200 |
| 07S | >200 | >200 | >200 | >200 |
| 07N | >200 | >200 | >200 | >200 |
| 198C | 83.5 (67.2–103.8) | 10.3 (7.9–13.4) | >200 | >200 |
| 198S | 105.6 (87.8–126.9) | 15.7 (11.6–21.2) | >200 | >200 |
| 198N | 74.3 (55.4–99.7) | 14.8 (11.8–18.6) | ≥200 | >200 |
| 27C | 44.1 (34.3–56.8) | 17.0 (13.4–21.6) | >200 | >200 |
| 27S | 146.7 (130.9–164.2) | 27.7 (26.8–28.6) | >200 | >200 |
| 27N | 130.5 (110.0–154.8) | 21.6 (17.3–27.0) | >200 | >200 |
| 40C | 58.4 (43.4–78.6) | 21.7 (12.0–38.9) | >200 | >200 |
| 40S | 156.2 (148.5–164.3) | >200 | >200 | >200 |
| 40N | >200 | 126.5 (89.1–179.4) | >200 | >200 |
| Oxytetracycline | 0.07 (0.05–0.09) | 12.4 (11.2–16.1) | 3.6 (2.6–4.9) | 0.15 (0.11–0.20) |

$IC_{50}$ values are expressed as CI95%. Values in parentheses correspond to the 95% confidence intervals calculated by non-linear regression analysis using GraphPad Prism.

Most samples demonstrated antibacterial activity, reducing *C. acnes* and *S. epidermidis* growth by more than 50% at 200 µg/mL. Consequently, a dose–response analysis was conducted to determine the $IC_{50}$ values. The $IC_{50}$ values for *S. epidermidis* were particularly notable, with sample 198C exhibiting the highest potency ($IC_{50}$: 10.3 µg/mL), closely matching the reference standard ($IC_{50}$: 12.4 µg/mL). Several other samples also showed strong antimicrobial activity, with $IC_{50}$ values ranging from 14.8 to 21.7 µg/mL, including 198N ($IC_{50}$: 14.8 µg/mL), 198S ($IC_{50}$: 15.7 µg/mL), 27C ($IC_{50}$: 17.0 µg/mL), 27N ($IC_{50}$: 21.6 µg/mL), and 40C ($IC_{50}$: 21.7 µg/mL). The inhibitory activity against *C. acnes* was

not so marked as against *S. epidermidis*; however, samples 27C ($IC_{50}$: 44.1 µg/mL), 40C ($IC_{50}$: 58.4 µg/mL), 198N ($IC_{50}$: 74.3 µg/mL), and 198C ($IC_{50}$: 83.5 µg/mL) showed high antimicrobial activity. Concerning *S. hominis*, extract 198N showed the highest activity, reducing its growth by 51%. None of the extracts inhibited *S. aureus* growth at 200 µg/mL.

### 3.4. Insights into Antimicrobial Mechanisms of Action

Given the high antimicrobial properties exhibited by some of the microalgae extracts, further investigation was conducted to explore the potential mechanisms underlying these effects, with focus on their capacity to disrupt membrane integrity (3.4.1) and to damage DNA (3.4.2).

#### 3.4.1. Membrane Damage

Membrane damage is a primary mechanism of action for many antimicrobial compounds, making it an essential target in the development of new therapies. The membrane damage induced by samples 40C (*S. armatus*) and 198C (*C. sorokiniana*) on *S. epidermidis* and *C. acnes* is depicted in Figures 2A and 2B, respectively.

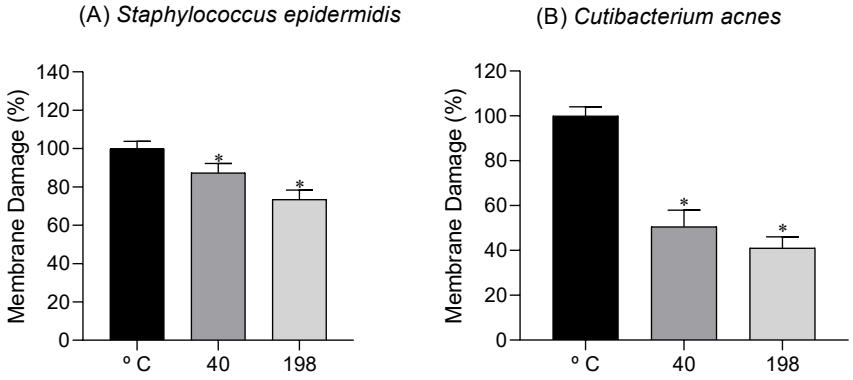


**Figure 2.** Membrane damage caused by the 40C (*Scenedesmus armatus*) and 198C (*Chlorella sorokiniana*) extracts (200 µg/mL; over 4 h for *S. epidermidis* and over 6 h for *C. acnes*) on *Staphylococcus epidermidis* (**A**) and *Cutibacterium acnes* (**B**). The values represent the mean ± std. error of mean (SEM). * Symbol represents significant differences (ANOVA, Dunnett's test, $p < 0.05$) when compared to control (thermic treatment at 100 °C).

The results indicate that the microalgae extracts cause significant membrane damage to both *S. epidermidis* and *C. acnes*. For *S. epidermidis*, sample 40C demonstrated the highest damaging capacity (87.3%), followed by 198C (73.5%). In contrast, the damage induced in *C. acnes* (Figure 2B) by samples 40C and 198C was lower, exhibiting a damage of 50.5% and 41.1%, respectively.

#### 3.4.2. DNA Damage

Studying the DNA-damaging potential of antimicrobial agents is vital for understanding how these compounds interfere with bacterial genetic material, which can lead to mutations and cell death. DNA damage is a key mechanism by which many antimicrobial agents exert their effects, disrupting replication and cellular functions. The DNA-damaging potential of samples 40C (*S. armatus*) and 198C (*C. sorokiniana*) is depicted in Figure 3A,B.

As shown in Figure 3, samples 40C and 198C induced remarkable DNA damage, suggesting that the antimicrobial effects mediated by these samples may be associated with DNA-damaging, particularly since these samples also impacted on cellular membranes.

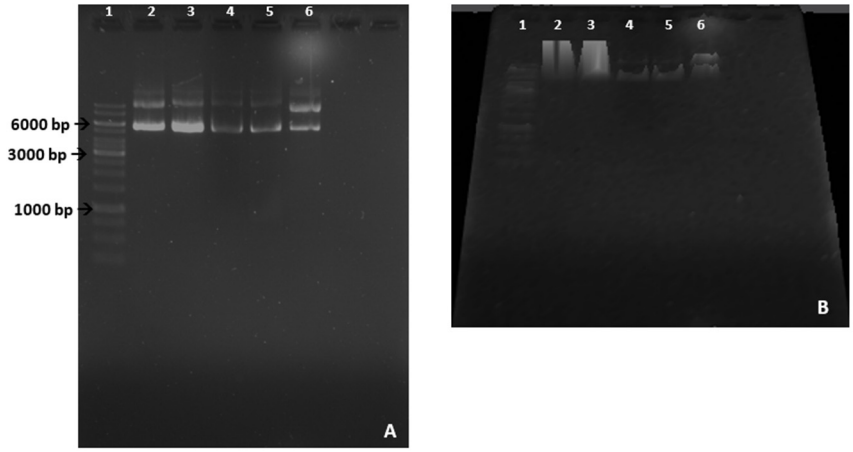


**Figure 3.** (**A**) Electrophoresis gel: 1—DNA Ladder; 2—DNA (100 ng); 3—DNA + DMSO; 4—DNA + sample 40C (*Scenedesmus armatus*; 2 mg/mL); 5—DNA + sample 198C (*Chlorella sorokiniana*; 2 mg/mL); 6—DNA + ciprofloxacin (1 µg/mL). Agarose at 0.8%, run at 85 V for 45 min. Images were obtained through a gel imaging system (Gel doc). The gel was visualized after gel-red staining and UV irradiation. The results are representative of three independent experiments. (**B**) 3D image of the same electrophoresis.

### *3.5. Chemical Screening of the Most Bioactive Extracts*

#### 3.5.1. UV-Vis Spectra

The UV-Vis spectra of the most bioactive samples, 40C (*S. armatus*) and 198C (*C. sorokiniana*), are depicted in Figure 4.

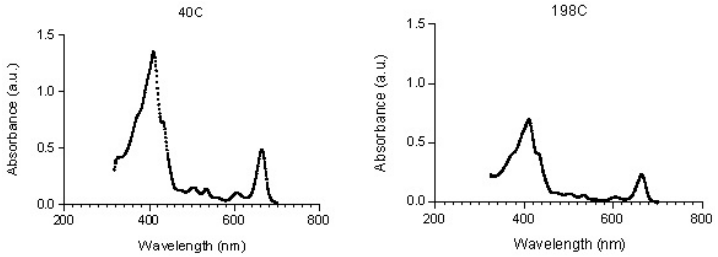


**Figure 4.** UV-Vis absorption spectra (200–800 nm) of the bioactive extracts 40C (*Scenedesmus armatus*) and 198C (*Chlorella sorokiniana*).

Some similarities are evident in the UV-Vis spectra of both samples, with absorption maxima in the range of 410–665 nm characteristic of pigments. Less intense peaks between 210 and 320 nm were also observed, suggesting the presence of other molecules such as phenolic compounds, α-tocopherol, and unsaturated fatty acids.

#### 3.5.2. $^{1}$H NMR Spectra

The chemical profile of the bioactive extracts 40C (*S. armatus*) and 198C (*C. sorokiniana*) was analyzed by $^{1}$H NMR, and the corresponding spectra are depicted in Figure 5.

A tentative identification of major compound groups was made for both spectra (Figure 5). It is possible to identify the diagnostic resonances of olefinic and allylic protons of unsaturated fatty acids (FA) at regions of $\delta_H$ 5.27–5.36 ppm and $\delta_H$ 2.08–2.04 ppm, respectively. The diagnostic region of polyunsaturated FA due to resonances of internal methylene protons attached to two double bonds appears at $\delta_H$ 2.78–2.92 ppm. The methylene protons directly attached to the carbonyl group of FA appear as a multiplet between $\delta_H$ 2.25 and 2.34 ppm. The methylene protons in the beta position in relation to the carbonyl group ($\delta_H$ 1.59–1.56 ppm) and the long-chain methylene protons of FA were found in the range of $\delta_H$ 1.28–1.33 ppm. The terminal methyl protons from omega-3

FA were confirmed by the appearance of a triplet at $\delta_H$ 0.97–0.93 ppm, while the signals assigned to the rest of FA were found at $\delta_H$ 0.88 ppm.

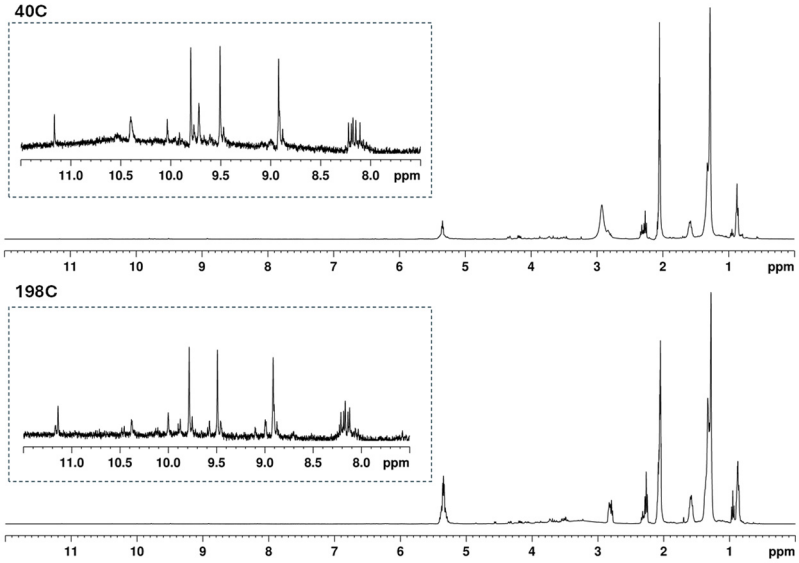


**Figure 5.** $^1$H NMR spectra (400 MHz) in acetone-$d_6$ of the bioactive fractions 40C (*Scenedesmus armatus*) and 198C (*Chlorella sorokiniana*).

As can be seen in the expanded spectra (7.50–11.50 ppm), besides the signals in the aliphatic and olefinic regions, carotenoids and chlorophylls also displayed signals of aromatic resonances (8.10–8.22 ppm). Aromatic proton resonances typically appear in the δ 6.0–8.5 ppm range, depending on substitution patterns and ring systems [57]. Additionally, chlorophylls could be spotted in the spectra from the isolated proton signals between δH 8.88 and 11.16 ppm. Signals observed in the δ 9–11 ppm region are consistent with deshielded protons in porphyrin-type macrocycles, such as those found in chlorophyll derivatives. Similar downfield signals have been reported in NMR studies of chlorophylls and pheophytins due to the strong ring current effects of the tetrapyrrolic system [58–61].

#### 3.5.3. LC-MS Data

Aiming to identify their fatty acid composition, the bioactive samples (40C and 198C) were also analyzed by LC-MS. Results are summarized in Tables S1 and S2 (Supporting Information).

As shown in Tables S1 and S2, unsaturated fatty acids (oleic, linolenic, linoleic), along with a saturated fatty acid (palmitic), are the most relatively abundant fatty acids in both samples. These are followed by palmitelaidic, stearic, and stearidonic acids. Stearidonic acid is significantly more abundant in the 40C sample compared to the 198C, indicating a higher presence of polyunsaturated fatty acids in the 40C sample. In contrast, margaric and myristic acids are detected in higher concentrations in sample 198C, suggesting an increased proportion of saturated fatty acids in this sample. Pelargonic, nonadecylic, and pentadecylic acids are present in lower concentrations in both samples, indicating their minimal contribution to the overall fatty acid profile. Notably, gadoleic acid is exclusively found in sample 40C, further differentiating the composition of the two samples, with 40C exhibiting a greater diversity of unsaturated fatty acids.

## 4. Discussion

Regarding species identification, although some pairs of strains were identified as belonging to the same species, these pairs did not perform equally well in the tests. This

variation is likely due to the strains being collected from different locations and/or at different times. After all, it is already known that the environment is one of the determining factors in the expression of a phenotype. Phenotypic plasticity is an evolutionary adaptation strategy that enhances a species' chances of survival. It can occur in the physiology, morphology, and biochemical characteristics of an individual [62]. These traits are directly associated with the bioactivities observed in microalgae extracts.

A possible explanation for the superior performance of *S. armatus* and *C. sorokiniana* lies in their metabolic capacity to produce higher amounts of antioxidant pigments, such as chlorophylls and carotenoids, and unsaturated fatty acids with recognized bioactivities [63]. Both species belong to the phylum Chlorophyta, which is known for its high metabolic plasticity and ecological adaptability to environmental stressors such as high radiation or nutrient limitation. Nitrogen deficiency and salinity are among the key environmental factors known to induce oxidative stress and trigger antioxidant responses in microalgae. These stressors can stimulate the biosynthesis and accumulation of bioactive compounds such as carotenoids, xanthophylls, and lipids [64]. In fact, nutrient limitation, particularly nitrogen deprivation, and salinity stress are two of the most commonly applied strategies to enhance the production of high-value metabolites in microalgae [65]. Nitrogen limitation, for instance, promotes lipid accumulation due to the redirection of metabolic pathways when this essential macronutrient is scarce. Similarly, salinity stress disrupts cellular homeostasis, prompting the organism to initiate protective mechanisms, including the increased production of lipids, carotenoids, and other secondary metabolites, primarily to mitigate oxidative damage intensified under such stress conditions [19]. This framework was the scientific basis for selecting nitrogen deficiency and salinity as stress factors in our study.

These stressors may activate biosynthetic pathways that enhance the production of protective secondary metabolites. Additionally, the fact that these strains were collected from distinct locations may have led to the selection of more metabolically specialized lineages, reinforcing the idea that environmental factors directly shape the observed bioactivity profiles.

This plasticity, in turn, is one of the factors responsible for the bioactivities exhibited by microalgae. In this sense, the increasing number of pathological conditions related to oxidative stress has led to a growing search for new sources of natural antioxidants. The potential of microalgae as a source of these ingredients is already well known due to the action of different compounds, including pigments such as carotenoids and chlorophylls [66]. Molecules such as $\beta$-carotene, lutein, and astaxanthin are widely reported for their antioxidant capacity. However, a molecule that also possesses antioxidant activity is often overlooked: chlorophyll. In addition to its primary function in photosynthesis, chlorophyll is capable of eliminating free radicals and reducing oxidative stress [66].

Although not traditionally associated with the antioxidant capacity of microalgae, chlorophyll has been gaining prominence in the cosmetic industry due to its potential to promote healthier skin [67]. In 2021, the global chlorophyll market was valued at US$252.19 million and is projected to reach US$504.10 million by 2030 [68]. Based on the findings thus far, the antioxidant activity observed in the extracts may be partially attributed to the presence of chlorophylls. Although the most active extracts, such as 40C and 198C, exhibited moderate DPPH radical scavenging capacities (22.6% and 20.7%, respectively), these values are consistent with those reported for crude natural extracts. In contrast, synthetic antioxidants like BHT commonly reach reduction levels above 75% [69], largely due to their pure, single-compound composition and highly specific mechanisms of action. Crude extracts, on the other hand, comprise a complex mixture of metabolites that may interact in additive or synergistic ways. However, such synergistic effects remain

hypothetical in the present study, as no experimental validation (e.g., compound isolation or combinatorial testing) was performed. Nevertheless, when considered alongside the results obtained from FRAP and superoxide scavenging assays, the data support the functional antioxidant potential of these extracts. Such broad-spectrum but moderate activity is often desirable in topical dermocosmetic applications, where gentler antioxidant mechanisms can contribute to skin protection without inducing irritation. However, preliminary LC-MS data also suggest the presence of other pigments, such as carotenoids, which are already recognized for their antioxidant properties.

One of the key characteristics of microalgae is their ability to harness sunlight for biomass production through photosynthesis. During this process, the cells accumulate various defense compounds to cope with challenges such as variations in nutrient availability or periods of light intensity, as excess light can induce oxidative stress. Carotenoids, such as astaxanthin and β-carotene, can act as important antioxidant agents by directly neutralizing free radicals, stimulating antioxidant enzyme activity, and activating transcription factors for genes involved in antioxidant production, among other functions [70]. Animal studies have already shown promising effects of microalgae-derived antioxidants in protecting the skin from oxidative damage caused by UV radiation, thereby preventing sunburn and premature aging. In addition, these antioxidants also help combat inflammation, such as in cases of acne, and contribute to overall improvement in skin health [71].

Distinct biological activities have already been reported for a wide variety of compounds produced by microalgae, including antimicrobial activities [15]. This is extremely important because these organisms have been revealed to be a renewable source of bioactive compounds. In the case of antibacterials, they hold particular significance as potential producers of undiscovered molecules that could be useful to combat microorganisms resistant to conventional drugs [72]. Among the most well-known microalgal compounds with antimicrobial activity are unsaturated fatty acids [73].

Studies involving *S. hominis* are relatively scarce, particularly those investigating the activity of microalgae extracts against this bacterium. *S. hominis* is a coagulase-negative *Staphylococcus* commonly found on human skin, where it plays a role in natural microbiota. However, it can become opportunistic, contributing to skin infections and even antibiotic-resistant strains in hospital settings. Research on microalgae-derived extracts and compounds has gained interest due to their antimicrobial and anti-inflammatory properties [70,74]. Certain microalgae species, such as *Chlorella* and *Scenedesmus* [74], have demonstrated activity against *Staphylococcus* species, suggesting the potential for combating *S. hominis* infections. Vahdati et al. [72] evaluated the antimicrobial capacity of green microalgae methanolic extracts and reported a minimum inhibitory concentration of 0.75 mg/mL against *S. aureus*, which is a concentration 3 times higher than those tested in the present work. Although extracts are generally a complex mixture of compounds, our data are in line with the literature, showing their relevance for possible application in the skin care industry.

Skin pathologies associated with *C. acnes* outbreaks are among the most prevalent, particularly in adolescents. This is primarily due to the overproduction of sebum by sebaceous glands, which creates an ideal environment for bacterial proliferation. The excessive sebum, combined with follicular hyperkeratinization and inflammation, contributes to conditions such as acne vulgaris. Additionally, *C. acnes* has been linked to other dermatological disorders, including folliculitis and certain forms of dermatitis [75].

*Cutibacterium acnes* is a Gram-positive, anaerobic bacterium naturally found on human skin, primarily in sebaceous follicles. Studies on counteracting *C. acnes* infections are crucial for developing effective acne treatments, especially as antibiotic resistance becomes a growing concern. Research focusing on alternative therapies, such as marine-derived

compounds that selectively target *C. acnes*, is of utmost relevance. In the case of *C. acnes*, previous studies have demonstrated the ability of macroalgae extracts to inhibit its growth [76], as well as the effectiveness of microalgae, such as *Arthrospira platensis*, in preventing *C. acnes* biofilm formation [77]. However, research on the antimicrobial potential of other microalgal species remains limited or largely unexplored. In the present work, sample 27C exhibited antibacterial activity against both targeted bacteria, with a particularly strong effect against *C. acnes*. The microalgae in question belong to the *Desmodesmus* genus, which has previously been reported to display antibacterial activity against *Staphylococcus aureus* (MIC of 31.25 μg/mL) and also against methicillin-resistant *Staphylococcus aureus* (MIC of 250 μg/mL) [78].

Regarding the mechanisms of action, the effects of both extracts on the cytoplasmic membrane and DNA offer valuable insights. The disruption of bacterial membrane integrity leads to leakage of cellular contents, loss of membrane potential, and ultimately bacterial death. In fact, this is the mechanism of action of commercial drugs such as polymyxins (e.g., polymyxin B and E) that target the outer cell membrane of Gram-negative bacteria and daptomycin, an antimicrobial peptide that targets the membrane of Gram-positive bacteria, causing membrane depolarization and bacterial cell death [79].

Specifically, polyunsaturated fatty acids (PUFAs) are highly susceptible to lipid peroxidation due to their multiple double bonds. This structural feature makes them prone to oxidative attack, leading to the formation of lipid peroxides and secondary reactive aldehydes (e.g., malondialdehyde and 4-hydroxynonenal). These reactive products can disrupt membrane integrity by increasing lipid bilayer disorder, altering membrane fluidity and permeability, and impairing membrane-bound proteins. Such changes can ultimately result in loss of membrane function and increased cellular vulnerability. In addition, lipid peroxidation products derived from PUFAs are known to interact with nucleic acids. Reactive aldehydes can form adducts with DNA bases and promote oxidative DNA lesions either directly or indirectly through the generation of reactive oxygen species. Therefore, the enrichment of specific PUFAs in the chemical profile may enhance susceptibility to oxidative stress, providing a plausible mechanistic link between the observed lipid composition and both membrane disruption and DNA damage [80–83].

Furthermore, natural antimicrobial compounds are biodegradable and less toxic to human cells and to the environment, making them promising candidates for developing sustainable and safer alternatives in combating bacterial infections, including opportunistic skin bacteria like *S. epidermidis* and *C. acnes*. Although further studies are required to fully elucidate the mechanisms of action involved in the demonstrated antimicrobial activity, the data presented here support the promising potential of microalgae, particularly the *Chlorella* and *Scenedesmus* genera, to produce valuable bioactive compounds that could inspire the development of novel antibacterial formulations to treat skin pathologies associated with microbiome imbalance.

The UV-Vis analysis showed that the absorption maxima of pigments and other microalgae components strongly depend on the type of solvent in which they are dissolved and, to a lesser extent, on the accuracy of the analytical equipment. On the other hand, it is important to note that absorption maxima reported in the literature generally refer to pure compounds, leading to some deviations when analyzing UV-Vis spectral data of crude extracts, making the equation derived from the Lambert–Beer law more complex.

The pigment's production by microalgae shows different results, depending on a set of factors as previously described by some authors [84,85]. Concerning our extracts, chlorophylls, in particular chlorophyll *a*, are present in both samples, but in greater amounts in sample 40C. Absorption maxima around 420 nm and 665 nm are attributed to this pigment, while the carotenoid absorption band is in the spectral range of 420–480 nm,

with absorption maxima of 440 and 470 nm [86]. Sample 40C also showed the highest antioxidant capacity, suggesting that chlorophyll could make an additional contribution to this activity. The $^{1}$H NMR spectra of both samples are very similar, and, overall, they are in accordance with data previously reported [87–89], showing that fatty acids (FAs) are the major metabolites produced by *C. sorokiniana* and *S. armatus*.

The phylum *Chlorophyta* (green algae), to which the microalgae studied here belong, possesses a great capacity to biosynthesize a diverse range of polyunsaturated fatty acids (PUFAs) and other lipids. In general, free fatty acids (FFAs), saturated and unsaturated fatty acids exhibit antibacterial activity against pathogens with a significant impact on human health, including *Escherichia coli*, *Pseudomonas aeruginosa*, *Klebsiella* spp., *Bacillus* spp., *S. aureus* and *S. epidermidis*. Although *S. hominis*, *S. epidermidis* and *C. acnes* are not yet as commonly associated with severe infections as *S. aureus*, their ability to produce biofilms raises significant concern due to the challenges these biofilms pose in treatment and eradication. The use of microalgae FAs targets areas where conventional drugs are ineffective or no longer effective. This is particularly important for preventing microbial colonization of medical equipment and for the topical treatment of hospital patients [90].

The genus *Scenedesmus* sp. has been described as having a high production of fatty acids, which is why it is widely used to produce biodiesel [91]. Likewise, the genus *Chlorella* sp. is known as a high producer of FA, and its FA composition is already well known [92]. These studies corroborate our findings. As for the composition of the fatty acids found, three of them are unsaturated (oleic, linolenic, and linoleic) and well known for their antibiotic activity, but also antioxidant and anti-aging activities, among many others [93]. However, in this sense, it is not possible to clearly state which compounds are responsible for the observed antioxidant and antibacterial capacities, as the extracts were not fractioned and purified. The two extracts showed very similar activity patterns and chemical characteristics, and it can be hypothesized that they could act individually or synergistically. To clarify this, further studies are needed to separate the compounds and to test their bioactivity individually.

## 5. Conclusions

Among the eight species of microalgae evaluated in this study, two of them stood out for their antioxidant and antibacterial capacities. The extracts of *Scenedesmus armatus* and *Chlorella sorokiniana* showed the best antioxidant results in two of the three methods evaluated. In the antibacterial test against *Staphylococcus epidermidis*, *C. sorokiniana* obtained an $IC_{50}$ value similar to that of the standard drug (oxytetracycline). On the other hand, *S. armatus* stood out in its antibacterial activity against *C. acnes*, although its $IC_{50}$ value was far from the value found for oxytetracycline. When the damage to the membrane of these bacteria was assessed, the results showed that both extracts caused significant damage, with greater expression in *S. epidermidis*. As for DNA, both extracts showed the same pattern of damage.

In addition, *S. armatus* and *C. sorokiniana* exhibited very similar chemical profiles, with a greater production of chlorophyll by *S. armatus*. The lipid profile revealed that, in *S. armatus*, the oleic and palmitic acids are the predominant fatty acids, while in *C. sorokiniana*, linolenic and linoleic acids are present in major amounts. Although the natural variability of microalgal metabolites may limit extract standardization, this challenge can be mitigated by using controlled cultivation systems and optimized protocols. Notably, the strains *S. armatus* and *C. sorokiniana* are considered suitable for large-scale production, supporting their potential integration into industrial bioprocesses. To the best of our knowledge, this is the first report on the dual antioxidant and antibacterial potential of Brazilian strains of microalgae cultivated under different stress conditions, expanding their biotechnological

relevance for dermocosmetic applications. From a practical perspective, the antioxidant and antibacterial profiles reported here support the incorporation of these crude extracts into topical formulations such as creams or gels for acne-prone or sensitive skin. Their activity against *C. acnes* and *S. epidermidis*, combined with the presence of beneficial lipids and pigments, reinforces their value as multifunctional ingredients. The data obtained here are in line with other publications, highlighting the potential of microalgae, especially of the *Scenedesmus* and *Chlorella* genera, to produce compounds with marked antioxidant and antibacterial activity. However, more studies are needed to elucidate which specific compounds perform these activities to target their application in new dermatological and/or cosmetic formulations. Furthermore, the integration of advanced analytical techniques, such as metabolomics, would greatly enhance the understanding of the bioactive profiles of these extracts and support the identification of key compounds responsible for their biological effects.

**Supplementary Materials:** The following supporting information can be downloaded at: https://www.mdpi.com/article/10.3390/app16042146/s1, Table S1: Relative fatty acid composition of sample 40C (*Scenedesmus armatus*) analyzed by LC-MS; Table S2: Relative fatty acid composition of sample 198C (*Chlorella sorokiniana*) analyzed by LC-MS.

**Author Contributions:** Conceptualization, C.A., J.S., G.B., A.R. and J.A.P.H.; methodology, É.A.R.B., J.S.H., P.S., A.M., S.P., H.G., M.M., K.S., P.M., T.I.L. and E.B.; validation, C.A., J.S., S.P. and A.M.; formal analysis, É.A.R.B., C.A., J.S. and A.M.; writing—original draft preparation, É.A.R.B., A.M. and S.P.; writing—review and editing, All authors; supervision, C.A., J.S., G.B., A.R. and J.A.P.H.; funding acquisition, C.A., J.S., G.B. and A.R. All authors have read and agreed to the published version of the manuscript.

**Funding:** This work was funded by the Portuguese Foundation for Science and Technology (FCT) through the strategic projects granted to MARE—Marine and Environmental Sciences Centre (UID/04292/2025, https://doi.org/10.54499/UID/PRR/04292/2025, Associate Laboratory ARNET (LA/P/0069/2020), and BioISI-Biosystems and Integrative Sciences Institute (UID/04046/2025, https://doi.org/10.54499/UID/04046/2025; FCT also funded this work through the project NEURONS4—New edge in the therapeutics of Parkinson's disease from seaweeds (2022.09196.PTDC; https://doi.org/10.54499/2022.09196.PTDC). This work was also supported by BEAP-MAR (EAPA_0032/2022) project through Interreg Atlantic Area, co-funded by the European Union and SEA-UP (DOI: https://doi.org/10.54499/2023.13029.PEX). FCT also funded this work through grants CEECINST/00060/2021/CP2902/CT0004 (Celso Alves, https://doi.org/10.54499/CEECINST/00060/2021/CP2902/CT0004), 2023.06590.CEECIND/CP2852/CT0002 (Joana Silva, https://doi.org/10.54499/2023.06590.CEECIND/CP2852/CT0002), and 2023.06631.CEECIND (Susete Pinteus).

**Data Availability Statement:** The data presented in this study are available on request from the corresponding author under the permission of the Syntalgae company.

**Acknowledgments:** The authors would like to acknowledge Universidade do Vale do Taquari-Univates, Conselho Nacional de Desenvolvimento Científico e Tecnológico (CNPq), and Syntalgae Research and Development for providing financial support. The authors would like to thank Syntalgae Research and Development for the technical support provided during the development of this work. The authors are very grateful for the financial support of the projects and programs described in the funding section.

**Conflicts of Interest:** The authors declare no conflicts of interest.

## References

1. Figueroa-Torres, G.M.; Bermejo-Padilla, E.; Wang, G.; Hilmisson, B.; Pittman, J.K.; Theodoropoulos, C. *Microalgae Strain Catalogue*, 4th ed.; University of Manchester: Manchester, UK, 2016; pp. 1–228.
2. Martínez Andrade, K.A.; Lauritano, C.; Romano, G.; Ianora, A. Marine microalgae with anti-cancer Properties. *Mar. Drugs* **2018**, *16*, 165. [CrossRef]

3. Ariede, M.B.; Candido, T.M.; Jacome, A.L.M.; Velasco, M.V.R.; de Carvalho, J.C.M.; Baby, A.R. Cosmetic attributes of algae—A review. *Algal Res.* **2017**, *25*, 483487. [CrossRef]
4. UNEP. Megadiverse Brazil: Giving Biodiversity an Online Boost. Available online: https://www.unep.org/news-and-stories/story/megadiverse-brazil-giving-biodiversity-online-boost (accessed on 15 October 2023).
5. Brazil Flora Group. Brazilian Flora 2020: Leveraging the power of a collaborative scientific network. *Taxon* **2022**, *71*, 178–198. [CrossRef]
6. Mendes, R.L.; Nobre, B.P.; Cardoso, M.T.; Pereira, A.P.; Palavra, A.F. Supercritical carbon dioxide extraction of compounds with pharmaceutical importance from microalgae. *Inorganica Chim. Acta* **2003**, *356*, 328–334. [CrossRef]
7. Plaza, M.; Cifuentes, A.; Ibáñez, E. In the search of new functional food ingredients from algae. *Trends Food Sci. Technol.* **2008**, *19*, 31–39. [CrossRef]
8. de Oliveira, D.T.; da Costa, A.A.F.; Costa, F.F.; da Rocha Filho, G.N.; do Nascimento, L.A.S. Advances in the biotechnological potential of Brazilian marine microalgae and cyanobacteria. *Molecules* **2020**, *25*, 2908. [CrossRef]
9. Saha, S.; Shukla, S.K.; Singh, H.R.; Singh, B.; Jha, S.K. Bioactive compounds from microalgae. In *An Integration of Phycoremediation Processes in Wastewater Treatment*; Elsevier: Amsterdam, The Netherlands, 2022; pp. 337–358. [CrossRef]
10. Qin, Y. Health benefits of bioactive seaweed substances. In *Handbook of Algal Science, Technology and Medicine*; Academic Press: Cambridge, MA, USA, 2020; pp. 455–466. [CrossRef]
11. Grice, E.A.; Segre, J.A. The skin microbiome. *Nat. Rev. Microbiol.* **2011**, *9*, 244–253. [CrossRef] [PubMed]
12. Zhang, Y.; Gao, Y.; Zeng, Y.; Zhang, J.; Wang, X.; Wang, J. Microbiome: Role in inflammatory skin diseases. *Front. Immunol.* **2024**, *15*, 1243042. [CrossRef]
13. Parlet, C.P.; Brown, M.M.; Horswill, A.R. Commensal Staphylococci Influence Staphylococcus aureus Skin Colonization and Disease. *Trends Microbiol.* **2019**, *27*, 497–507. [CrossRef]
14. Laux, C.; Peschel, A.; Krismer, B. Staphylococcus aureus colonization of the human nose and interaction with other microbiome members. *Microbiol. Spectr.* **2019**, *7*, 1–10. [CrossRef]
15. Levasseur, W.; Perré, P.; Pozzobon, V. A review of high value-added molecules production by microalgae in light of the classification. *Biotechnol. Adv.* **2020**, *41*, 107–545. [CrossRef]
16. Jiang, S.; Zheng, B.; Ding, W.; Lv, L.; Ji, J.; Zhang, H.; Xiao, Y.; Li, L. Whole-Genome Sequence of Staphylococcus hominis, an Opportunistic Pathogen. *J. Bacteriol.* **2012**, *194*, 17. [CrossRef] [PubMed]
17. Becker, K.; Skov, R.L.; von Eiff, C. Staphylococcus, Micrococcus, and other catalase-positive cocci. In *Manual of Clinical Microbiology*; ASM Press: Washington, DC, USA, 2015; pp. 354–382. [CrossRef]
18. Miyazaki, A.N.; Salles, M.J.C.; Gonçalves, G.V.; Conte, L.H.G.; de Oliveira, T.G.; Santili, A.B.N.; Kurihara, M.N.L.; Santos, I.N.M.; da Silva, L.A. Detecção de Cutibacterium acnes em amostras de tecidos de cirurgias limpas primárias do ombro–Parte II. *Rev. Bras. Ortop.* **2023**, *58*, 257–264. [CrossRef] [PubMed]
19. Rinaldi, K.; Senhorinho, G.N.A.; Laamanen, C.A.; Scott, J.A. A review of extremophilic microalgae: Impacts of experimental cultivation conditions for the production of antimicrobials. *Algal Res.* **2024**, *78*, 103427. [CrossRef]
20. Alsenani, F.; Tupally, K.; Chua, E.T.; Eltanahy, E.; Alsufyani, H.; Parekh, H.S.; Schenk, P.M. Evaluation of microalgae and cyanobacteria as potential sources of antimicrobial compounds. *Saudi Pharm. J.* **2020**, *28*, 1834–1841. [CrossRef]
21. Borowitzka, M.A. High-value products from microalgae—Their development and commercialisation. *J. Appl. Phycol.* **2013**, *25*, 743–756. [CrossRef]
22. Brennan, L.; Owende, P. Biofuels from microalgae—A review of technologies for production, processing, and extractions of biofuels and co-products. *Renew. Sustain. Energy Rev.* **2010**, *14*, 557–577. [CrossRef]
23. Díaz, K.C. Biotecnología de microalgas como fuente de diversos compuestos de interés para la industria farmacéutica y alimentaria. *Vitae* **2012**, *19*, 76–77.
24. de Luca, M.; Pappalardo, I.; Limongi, A.R.; Viviano, E.; Radice, R.P.; Todisco, S.; Martelli, G.; Infantino, V.; Vassallo, A. Lipids from microalgae for cosmetic applications. *Cosmetics* **2021**, *8*, 52. [CrossRef]
25. Matos, A.P. Advances in microalgal research in Brazil. *Braz. Arch. Biol. Technol.* **2021**, *64*, e21200531. [CrossRef]
26. Bischoff, H.W. *Phycological Studies. IV. Some Algae from Enchanted Rock and Related Algal Species*; University of Texas Publication: Austin, TX, USA, 1963; p. 95.
27. Starr, R.C.; Zeikus, J.A. UTEX—The culture collection of algae at the University of Texas at Austin 1993 list of cultures 1. *J. Phycol.* **1993**, *29*, 1–106. [CrossRef]
28. Andersen, R.A. *Algal Culturing Techniques*; Academic Press: Cambridge, MA, USA, 2005.
29. Kuhl, A.; Lorenzen, H. Hmdling and culturing of Chlorella. In *Methods in Cell Biology*; Academic Press: Cambridge, MA, USA, 1964; pp. 159–187. [CrossRef]
30. Stanier, R.Y.; Kunisawa, R.; Mandel, M.; Cohen-Bazire, G. Purification and properties of unicellular blue-green algae (order Chroococcales). *Bacteriol. Rev.* **1971**, *35*, 171–205. [CrossRef]

31. Rippka, R.; Herdman, H. *Pasteur Culture Collection of Cyanobacteria: Catalogue and Taxonomic Handbook. I. Catalogue of Strains*; Institut Pasteur: Paris, France, 1992; Volume 1, p. 13.
32. Sueoka, N. Mitotic replication of deoxyribonucleic acid in Chlamydomonas reinhardi. *Proc. Natl. Acad. Sci. USA* **1960**, *46*, 83. [CrossRef]
33. Gorman, D.S.; Levine, R.P. Cytochrome f and plastocyanin: Their sequence in the photosynthetic electron transport chain of Chlamydomonas reinhardi. *Proc. Natl. Acad. Sci. USA* **1965**, *54*, 1665. [CrossRef]
34. Harris, E.H. *The Chlamydomonas Sourcebook*, 1st ed.; Academic Press: San Diego, CA, USA, 1989.
35. Slocombe, S.P.; Zhang, Q.; Ross, M.; Anderson, A.; Thomas, N.J.; Lapresa, A.; Rad-Menéndez, C.; Campbell, C.N.; Black, K.D.; Stanley, M.S.; et al. Unlocking nature's treasure-chest: Screening for oleaginous algae. *Sci. Rep.* **2015**, *5*, 9844. [CrossRef]
36. Bicudo, C.E.d.M.; Menezes, M. *Gêneros de Algas de Águas Continentais do Brasil*, 2nd ed; Rima: São Carlos, Brazil, 2006.
37. Murray, M.G.; Thompson, W.F. Rapid isolation of high molecular weight plant DNA. *Nucleic Acids Res.* **1980**, *8*, 4321–4326. [CrossRef]
38. Asker, D.; Awad, T.S. Isolation and characterization of a novel lutein-producing marine microalga using high throughput screening. *Food Res. Int.* **2019**, *116*, 660–667. [CrossRef]
39. Moon-van der Staay, S.Y.; van der Staay, G.W.M.; Guillou, L.; Vaulot, D.; Claustre, H.; Medlin, L.K. Abundance and diversity of prymnesiophytes in the picoplankton coμmunity from the equatorial Pacific Ocean inferred from 18S rDNA sequences. *Limnol. Oceanogr.* **2000**, *45*, 98–109. [CrossRef]
40. White, T.J.; Bruns, T.; Lee, S.; Taylor, J. Amplification and direct sequencing of fungal ribosomal RNA genes for phylogenetics. In *PCR Protocols: A Guide to Methods and Applications*; Academic Press: New York, NY, USA, 1990; Volume 18, pp. 315–322. [CrossRef]
41. Radha, S.; Fathima, A.A.; Iyappan, S.; Ramya, M. Direct colony PCR for rapid identification of varied microalgae from freshwater environment. *J. Appl. Phycol.* **2013**, *25*, 609–613. [CrossRef]
42. Fawley, M.W.; Fawley, K.P. Identification of Eukaryotic Microalgal Strains. *J. Appl. Phycol.* **2020**, *32*, 2699–2709. [CrossRef] [PubMed] [PubMed Central]
43. Cherdchukeattisak, P.; Fraser, P.D.; Purton, S.; Brocklehurst, T.W. Detection and enhancement of ketocarotenoid accumulation in the newly isolated sarcinoid green microalga Chlorosarcinopsis PY02. *Biology* **2018**, *7*, 17. [CrossRef]
44. Khona, D.K.; Shirolikar, S.M.; Gawde, K.K.; Hom, E.; Deodhar, M.A.; D'Souza, J.S. Characterization of salt stress-induced palmelloids in the green alga, Chlamydomonas reinhardtii. *Algal Res.* **2016**, *16*, 434448. [CrossRef]
45. Lobina, D.V.; Zenteno, S.T.; Arce, M.M.; Gómez, A.G.A. *Métodos y Herramientas Analíticas en la Evaluación de la Biomasa Microalgal*, 2nd ed.; Centro de Investigaciones Biológicas del Noroeste: La Paz, Mexico, 2017.
46. Brand-Williams, W.; Cuvelier, M.E.; Berset, C. Use of a free radical method to evaluate antioxidant activity. *LWT-Food Sci. Technol.* **1995**, *28*, 25–30. [CrossRef]
47. Silva, J.; Alves, C.; Freitas, R.; Martins, A.; Pinteus, S.; Ribeiro, J.; Gaspar, H.; Alfonso, A.; Pedrosa, R. Antioxidant and Neuroprotective Potential of the Brown Seaweed Bifurcaria bifurcata in an in vitro Parkinson's Disease Model. *Mar. Drugs* **2019**, *17*, 85. [CrossRef]
48. Benzie, I.F.F.; Strain, J.J. The ferric reducing ability of plasma (FRAP) as a measure of "antioxidant power": The FRAP assay. *Anal. Biochem.* **1996**, *239*, 70–76. [CrossRef] [PubMed]
49. Bora, K.S.; Sharma, A. Evaluation of antioxidant and free-radical scavenging potential of Artemisia absinthium. *Pharm. Biol.* **2011**, *49*, 1216–1223. [CrossRef]
50. Susano, P.; Silva, J.; Alves, C.; Martins, A.; Gaspar, H.; Pinteus, S.; Mouga, T.; Goettert, M.I.; Petrovski, Ž.; Branco, L.B.; et al. Unravelling the dermatological potential of the brown seaweed Carpomitra costata. *Mar. Drugs* **2021**, *19*, 135. [CrossRef] [PubMed]
51. Pinteus, S.; Lemos, M.F.L.; Simões, M.; Alves, C.; Silva, J.; Gaspar, H.; Martins, A.; Rodrigues, A.; Pedrosa, R. Marine invasive species for high-value products' exploration–Unveiling the antimicrobial potential of Asparagopsis armata against human pathogens. *Algal Res.* **2020**, *52*, 102091. [CrossRef]
52. Saha, S.K.; Hayes, K.; Moane, S.; Murray, P. Tagging of biomolecules with deuterated water (D2O) in commercially important microalgae. *Biotechnol. Lett.* **2013**, *35*, 1067–1072. [CrossRef]
53. Saitou, N.; Nei, M. The neighbor-joining method: A new method for reconstructing phylogenetic trees. *Mol. Biol. Evol.* **1987**, *4*, 406–425. [CrossRef]
54. Felsenstein, J. Confidence limits on phylogenies: An approach using the bootstrap. *Evolution* **1985**, *39*, 783–791. [CrossRef]
55. Tamura, K.; Nei, M.; Kumar, S. Prospects for inferring very large phylogenies by using the neighbor-joining method. *Proc. Natl. Acad. Sci. USA* **2004**, *101*, 11030–11035. [CrossRef] [PubMed]
56. Tamura, K.; Stecher, G.; Kumar, S. MEGA 11: Molecular Evolutionary Genetics Analysis Version 11. *Mol. Biol. Evol.* **2021**, *38*, 3022–3027. [CrossRef]
57. Claridge, T.D.W. *High-Resolution NMR Techniques in Organic Chemistry*, 3rd ed.; Elsevier: Amsterdam, The Netherlands, 2016; ISBN 9780080999869, 9780080999937 (eBook).

58. Abraham, R.J.; Smith, K.M. NMR spectra of porphyrins. 21. Applications of the ring-current model to porphyrin and chlorophyll aggregation. *J. Am. Chem. Soc.* **1983**, *105*, 5734–5741. [CrossRef]
59. Abraham, R.J.; Smith, K.M.; Goff, D.A.; Lai, J.J. NMR Spectra of Porphyrins. 18. A Ring-Current Model for Chlorophyll Derivatives. *J. Am. Chem. Soc.* **1982**, *104*, 4332–4337. [CrossRef]
60. Gjuroski, I.; Furrer, J.; Vermathen, M. Probing the Interactions of Porphyrins with Macromolecules Using NMR Spectroscopy Techniques. *Molecules* **2021**, *26*, 1942. [CrossRef] [PubMed]
61. Dijkema, C.; Searle, G.F.; Schaafsma, T.J. 500 MHz $^{1}$H NMR of chlorophylls in the major light-harvesting chlorophyll-protein complex of photosystem II. *Biochem. Biophys. Res. Commun.* **1988**, *157*, 1085–1092. [CrossRef]
62. González-Hourcade, M.; Fernando, D.; Gentili, F. Morphological and cellular organization of green microalgae to cope with cold stress in subarctic environment. *Algal Res.* **2023**, *75*, 103254. [CrossRef]
63. Mititelu, M.; Lupuliasa, D.; Neacșu, S.M.; Olteanu, G.; Busnatu, Ș.S.; Mihai, A.; Popovici, V.; Măru, N.; Boroghină, S.C.; Mihai, S.; et al. Polyunsaturated Fatty Acids and Human Health: A Key to Modern Nutritional Balance in Association with Polyphenolic Compounds from Food Sources. *Foods* **2025**, *14*, 46. [CrossRef]
64. Montero-Lobato, Z.; Vázquez, M.; Navarro, F.; Fuentes, J.L.; Bermejo, E.; Garbayo, I.; Vílchez, C.; Cuaresma, M. Chemically-Induced Production of Anti-Inflammatory Molecules in Microalgae. *Mar. Drugs* **2018**, *16*, 478. [CrossRef]
65. Ren, Y.; Sun, H.; Deng, J.; Huang, J.; Chen, F. Carotenoid Production from Microalgae: Biosynthesis, Salinity Responses and Novel Biotechnologies. *Mar. Drugs* **2021**, *19*, 713. [CrossRef]
66. Pereira, L.; Cotas, J.; Valado, A. Antioxidants from microalgae and their potential impact on human well-being. *Explor. Drug Sci.* **2024**, *2*, 292–321. [CrossRef]
67. Martínez-Ruiz, M.; Martínez-González, C.A.; Kim, D.-H.; Santiesteban-Romero, B.; Reyes-Pardo, H.; Villaseñor-Zepeda, K.R.; Meléndez-Sánchez, E.R.; Ramírez-Gamboa, D.; Díaz-Zamorano, A.L.; Sosa-Hernández, J.E.; et al. Microalgae Bioactive Compounds to Topical Applications Products—A Review. *Molecules* **2022**, *27*, 3512. [CrossRef] [PubMed]
68. Águila-Carricondo, P.; de La Roche Cadavid, J.P.; Galán, P.L.; Bautista, L.F.; Vicente, G. New green biorefineries from cyanobacterial-microalgal consortia: Production of chlorophyll-rich extracts for the cosmetic industry and sustainable biogas. *J. Clean. Prod.* **2023**, *429*, 139652. [CrossRef]
69. Sathasivam, R.; Ki, J.-S. A Review of the Biological Activities of Microalgal Carotenoids and Their Potential Use in Healthcare and Cosmetic Industries. *Mar. Drugs* **2018**, *16*, 26. [CrossRef]
70. Choo, W.T.; Teoh, M.L.; Phang, S.M.; Convey, P.; Yap, W.H.; Goh, B.H.; Beardall, J. Microalgae as potential anti-inflammatory natural product against human inflammatory skin diseases. *Front. Pharmacol.* **2020**, *11*, 1086. [CrossRef]
71. Shaima, A.F.; Yasin, N.H.M.; Ibrahim, N.; Takriff, M.S.; Gunasekaran, D.; Ismaeel, M.Y.Y. Unveiling antimicrobial activity of microalgae Chlorella sorokiniana (UKM2), Chlorella sp. (UKM8) and Scenedesmus sp. (UKM9). *Saudi J. Biol. Sci.* **2022**, *29*, 1043–1052. [CrossRef]
72. Vahdati, S.N.; Behboudi, H.; Tavakoli, S.; Aminian, F.; Ranjbar, R. Antimicrobial potential of the Green Microalgae isolated from the Persian Gulf. *Iran. J. Public Health* **2022**, *51*, 1134. [CrossRef]
73. Hernández-Urcera, J.; Romero, A.; Cruz, P.; Vasconcelos, V.; Figueras, A.; Novoa, B.; Rodríguez, F. Screening of microalgae for bioactivity with antiviral, antibacterial, anti-inflammatory and anti-cancer assays. *Biology* **2024**, *13*, 255. [CrossRef]
74. Pina-Pérez, M.C.; Rivas, A.; Martínez, A.; Rodrigo, D. Antimicrobial potential of macro and microalgae against pathogenic and spoilage microorganisms in food. *Food Chem.* **2017**, *235*, 34–44. [CrossRef]
75. Mayslich, C.; Grange, P.A.; Dupin, N. Cutibacterium acnes as an opportunistic pathogen: An update of its virulence-associated factors. *Microorganisms* **2021**, *9*, 303. [CrossRef]
76. Januário, A.P.; Félix, C.; Félix, R.; Shiels, K.; Murray, P.; Valent, P.; Lemos, M.F.L. Exploring the Therapeutical Potential of Asparagopsis armata Biomass: A Novel Approach for Acne Vulgaris Treatment. *Mar. Drugs* **2024**, *22*, 489. [CrossRef]
77. Lemoine, V.; Bernard, C.; Leman-Loubière, C.; Clément-Larosière, B.; Girardot, M.; Boudesocque-Delaye, L.; Munnier, E.; Imbert, C. Nanovectorized microalgal extracts to fight Candida albicans and Cutibacterium acnes Biofilms: Impact of dual-species conditions. *Antibiotics* **2020**, *9*, 279. [CrossRef]
78. Arguelles, E.D.L.R.; Laurena, A.C.; Martinez-Goss, M.R.; Monsalud, R.G. Antibacterial activity, total phenolic content and antioxidant capacity of a green microalga Desmodesmus sp. (U-AU2) from Los Baños, Laguna (Philippines). *J. Nat. Stud.* **2017**, *16*, 1–13.
79. Ma, Y.; Chang, X.; Zhang, S.; Zhang, P.; Guo, T.; Zhang, X.; Kong, Y.; Ma, S. New broad-spectrum and potent antibacterial agents with dual-targeting mechanism: Promoting FtsZ polymerization and disrupting bacterial membranes. *Eur. J. Med. Chem.* **2024**, *263*, 115930. [CrossRef]
80. Michael, S.M.; Jimena, R.; Jennifer, L.W. Polyunsaturated Fatty Acids Drive Lipid Peroxidation during Ferroptosis. *Cells* **2023**, *12*, 804. [CrossRef]

81. Kodali, S.T. Chapter 5: Oxidative Lipidomics: Analysis of Oxidized Lipids and Lipid Peroxidation in Biological Systems with Relevance to Health and Disease. In *Measuring Oxidants and Oxidative Stress in Biological Systems*; Berliner, L.J., Parinandi, N.L., Eds.; Springer: Cham, Switzerland, 2020. [CrossRef]
82. Suda, A.; Abdulaziz, B.; Yamamoto, Y.; Shima, H.; Saiki, Y.; Pan, Y.; Jin, Y.; Sun, J.; Low, Y.L.C.; Suzuki, C.; et al. Polyunsaturated fatty acids-induced ferroptosis suppresses pancreatic cancer growth. *Sci. Rep.* **2024**, *14*, 4409. [CrossRef]
83. Balakrishnan, M.; Anne, K.; Kenworthy, A.K. Lipid Peroxidation Drives Liquid–Liquid Phase Separation and Disrupts Raft Protein Partitioning in Biological Membranes. *J. Am. Chem. Soc.* **2024**, *146*, 1374–1387. [CrossRef] [PubMed]
84. Aizpuru, A.; Gonzalez-Sanchez, A. Traditional and new trend strategies to enhance pigment contents in microalgae. *World J. Microbiol. Biotechnol.* **2024**, *40*, 272. [CrossRef] [PubMed]
85. Hotos, G.N. Quantity and Quality of Light on Growth and Pigment Content of Dunaliella sp. and Anabaena sp. Cultures and the Use of Their Absorption Spectra as a Proxy Method for Assessment. *J. Mar. Sci. Eng.* **2023**, *11*, 1673. [CrossRef]
86. Bazarnova, J.; Smyatskaya, Y.; Shlykova, A.; Balabaev, A.; Đurović, S. Obtaining Fat-Soluble Pigments—Carotenoids from the Biomass of Chlorella Microalgae. *Appl. Sci.* **2022**, *12*, 3246. [CrossRef]
87. Caprara, C.d.S.C.; Mathias, T.K.; Santos, M.d.F.C.; D'Oca, M.G.M.; D'Oca, C.d.R.M.; Roselet, F.; Abreu, P.C.; Ramos, D.F. Application of 1HR-MAS NMR-Based Metabolite Fingerprinting of Marine Microalgae Metabolites. *Metabolites* **2023**, *13*, 202. [CrossRef] [PubMed]
88. Aguilera-Saez, L.M.; Abreu, A.C.; Camacho-Rodríguez, J.; Gonzalez-Lopez, C.V.; Ceron-García, M.C.; Fernandez, I. NMR Metabolomics as an Effective Tool to Unravel the Effect of Light Intensity and Temperature on the Composition of the Marine Microalgae Isochrysis galbana. *J. Agric. Food Chem.* **2019**, *67*, 3879–3889. [CrossRef]
89. Bustamam, M.S.A.; Pantami, H.A.; Azizan, A.; Shaari, K.; Min, C.C.; Abas, F.; Nagao, N.; Maulidiani, M.; Banerjee, S.; Sulaiman, F.; et al. Complementary Analytical Platforms of NMR Spectroscopy and LCMS Analysis in the Metabolite Profiling of Isochrysis galbana. *Mar. Drugs* **2021**, *19*, 139. [CrossRef]
90. Ilieva, Y.; Zaharieva, M.M.; Kroumov, A.D.; Najdenski, H. Antimicrobial and Ecological Potential of Chlorellaceae and Scenedesmaceae with a Focus on Wastewater Treatment and Industry, Fermentation. *Fermentation* **2024**, *10*, 341. [CrossRef]
91. Apandi, N.M.; Muhamad, M.S.; Mohamed, R.M.S.R.; Sunar, N.M.; Al-Gheethi, A.; Gani, P.; Rahman, F.A. Optimizing of microalgae Scenedesmus sp. biomass production in wet market wastewater using response surface methodology. *Sustainability* **2021**, *13*, 2216. [CrossRef]
92. Kalwani, M.; Kumari, A.; Rudra, S.G.; Chhabra, D.; Pabbi, S.; Shukla, P. Application of ANN-MOGA for nutrient sequestration for wastewater remediation and production of polyunsaturated fatty acid (PUFA) by Chlorella sorokiniana MSP1. *Chemosphere* **2024**, *349*, 140835. [CrossRef]
93. Chen, W.; Li, T.; Du, S.; Chen, H.; Wang, Q. Microalgal polyunsaturated fatty acids: Hotspots and production techniques. *Front. Bioeng. Biotechnol.* **2023**, *11*, 1146881. [CrossRef]